

Mechanism of Boron-Catalyzed *N*-Alkylation of Amines with Carboxylic Acids

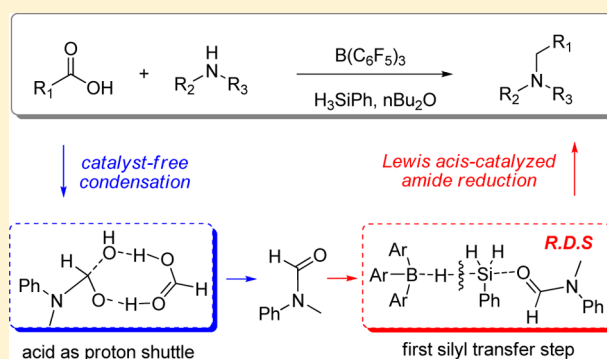
Qi Zhang,[†] Ming-Chen Fu,[†] Hai-Zhu Yu,^{*,‡} and Yao Fu^{*,†}

[†]Hefei National Laboratory for Physical Sciences at the Microscale, iChEM, CAS Key Laboratory of Urban Pollutant Conversion, Anhui Province Key Laboratory of Biomass Clean Energy, Department of Chemistry, University of Science and Technology of China, Hefei 230026, People's Republic of China

[‡]Department of Chemistry and Centre for Atomic Engineering of Advanced Materials, Anhui University, Hefei 230601, China

Supporting Information

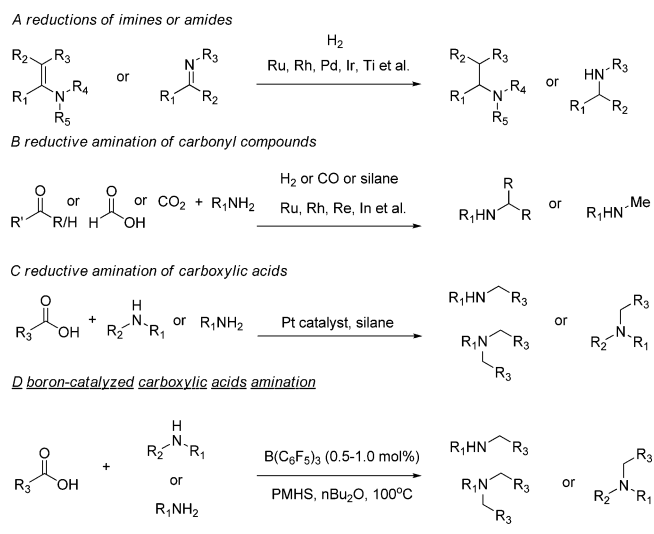
ABSTRACT: Mechanistic study has been carried out on the B(C₆F₅)₃-catalyzed amine alkylation with carboxylic acid. The reaction includes acid-amine condensation and amide reduction steps. In condensation step, the catalyst-free mechanism is found to be more favorable than the B(C₆F₅)₃-catalyzed mechanism, because the automatic formation of the stable B(C₆F₅)₃-amine complex deactivates the catalyst in the latter case. Meanwhile, the catalyst-free condensation is constituted by nucleophilic attack and the indirect H₂O-elimination (with acid acting as proton shuttle) steps. After that, the amide reduction undergoes a Lewis acid (B(C₆F₅)₃)-catalyzed mechanism rather than a Brønsted acid (B(C₆F₅)₃-coordinated HCOOH)-catalyzed one. The B(C₆F₅)₃-catalyzed reduction includes twice silyl-hydride transfer steps, while the first silyl transfer is the rate-determining step of the overall alkylation catalytic cycle. The above condensation–reduction mechanism is supported by control experiments (on both temperature and substrates). Meanwhile, the predicted chemoselectivity is consistent with the predominant formation of the alkylation product (over disilyl acetal product).



1. INTRODUCTION

N-Alkylated amines are ubiquitous structures in organic synthesis, pharmaceuticals, and biological systems.¹ Given the significance of these structures, developing straightforward and economic synthetic methods has become an important research topic.² As compared to the traditional substitution reactions of amines with hazardous alkyl halides,³ transition metal-catalyzed amine alkylation has recently attracted extensive interest.⁴ In recent years, Rh,⁵ Ir,⁶ Ru,⁷ Pd,⁸ etc., -catalyzed hydrogenative reduction of imines and enamines has become a powerful strategy to prepare *N*-alkylated amines (Scheme 1A). However, the substrates (imine and enamine) always require additional preparation from carbonyl compounds. With H₂, CO, or silane as reductants, Rh,⁹ Ir,¹⁰ Ru,¹¹ Re,¹² Fe,¹³ etc., -catalyzed reductive amination of carbonyl compounds¹⁴ (aldehydes, ketones, formic acid, and CO₂) provides a more straightforward method (Scheme 1B). For example, Beller's group¹⁵ successfully achieved the Pt-catalyzed alkylation of the more stable and available carboxylic acid substrates (Scheme 1C). In this context, our group recently reported a metal-free amine alkylation reaction using B(C₆F₅)₃ as catalyst and silane as reductant (Scheme 1D).¹⁶ The alkylation of various aromatic and aliphatic amines with formic acid and general carboxylic acid was achieved. In addition, three important commercialized drug molecules, Butenafine, Cinacalcet, and Piribedil, were easily synthesized through this method.¹⁶

Scheme 1. Synthetic Methods of *N*-Alkylated Amines



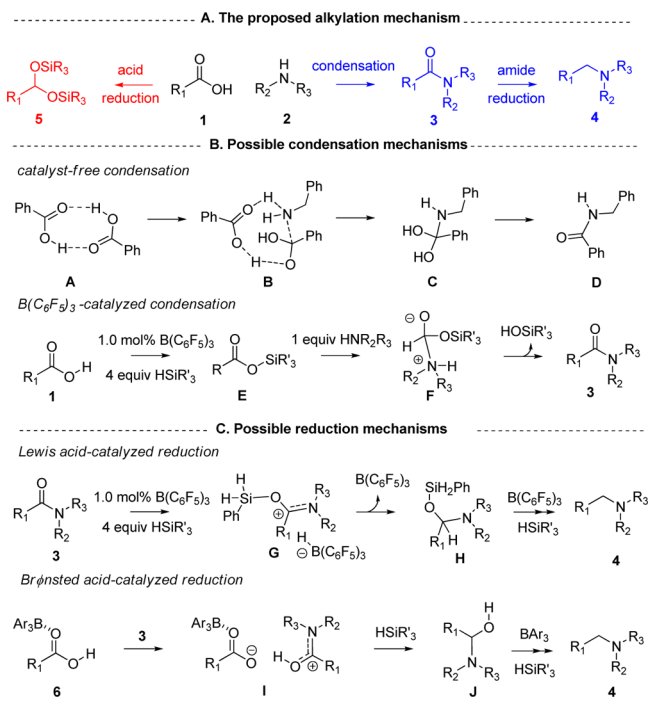
In studying the mechanism of the B(C₆F₅)₃-catalyzed amine alkylation, the control experiments indicate that amide is the possible intermediate, rather than aldehyde or alcohol.¹⁶

Received: April 8, 2016

Published: July 21, 2016

Accordingly, we proposed that carboxylic acid **1** and amine **2** first undergo condensation to generate amide **3**. Reduction of **3** then occurs to give the alkylation product **4** (Scheme 2A).

Scheme 2. (A) Possible Mechanisms of the Boron-Catalyzed Amine Alkylation and Acid Reduction; (B) Possible Condensation Mechanisms; and (C) Possible Reduction Mechanisms



Nonetheless, there are still some unsolved mechanistic problems. First, the detailed mechanism of the condensation is unclear. According to Whiting's recent study on the condensation reaction between benzoic acid and phenylethylamine,¹⁷ the mechanism mainly undergoes the acid dimerization, nucleophilic attack (with one carboxylic acid acting as proton acceptor), and H₂O-elimination steps (catalyst-free mechanism, Scheme 2B). On the other hand, Yamamoto^{18a} and Brookhart^{18b} et al. suggest that B(C₆F₅)₃-catalyzed condensation between carboxylic acid and amine might start with a rapid silane-carboxylic acid interaction, and the formed silyl ester then reacts with amine to generate the amide (B(C₆F₅)₃-catalyzed system, Scheme 2B).¹⁹ Both of these two mechanisms are plausible for the condensation step in our reaction system. Second, the mechanism of amide reduction is uncertain. According to the recent studies,^{20–24} either the Lewis acid or the Brønsted acid (B(C₆F₅)₃-coordinated acid) might catalyze the reduction of the carbonyl group (Scheme 2C). Third, the acid was found to be easily reduced to disilyl acetal **5** under the B(C₆F₅)₃-catalyzed system (Scheme 2A),¹⁸ whereas no disilyl acetal product was observed in our system. The origin for the interesting chemoselectivity is worth clarification. To solve these problems, we carried out combined theoretical and experimental mechanistic studies on the reaction shown in Scheme 1D.

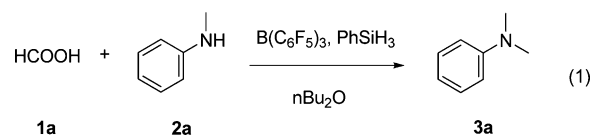
2. COMPUTATIONAL METHODS

The Gaussian 09 suite of program²⁵ was used for calculations in this study. The B3LYP^{26–28} method combined with the 6-31G* basis set and SMD model²⁹ was used for geometry optimization in dibutylether

solvent (consistent with our experiments¹⁶). To get the thermodynamic corrections of Gibbs free energy and verify the stationary points to be local minima or saddle points, we conducted frequency analysis at the same level with optimization. For all transition states, we performed the intrinsic reaction coordinate (IRC) analysis to confirm that they connect the correct reactants and products on the potential energy surfaces.³⁰ The M06-2X³¹/6-311++G** method with the SMD²⁹ model was used for the solution-phase single-point energy calculations of all of these stationary points (with dibutylether solvent). All energetics involved in this study are calculated by adding the Gibbs free energy correction calculated at B3LYP/6-31G* and the single-point energy calculated via the M06-2X/6-311++G** method.³²

3. RESULTS AND DISCUSSION

3.1. Model Reaction. In accordance with our experimental work,¹⁶ the generation of dimethylaniline **3a** by the reaction of formic acid **1a** with methylaniline **2a** (eq 1) is chosen as the model reaction. B(C₆F₅)₃, PhSiH₃, and *n*Bu₂O are used as catalyst, reductant, and solvent, respectively.



3.2. Mechanism of the Amine Alkylation. Efforts were first put into examining the energy demands of the mechanism of the amine alkylation. In this mechanism, **1a** and **2a** first undergo condensation to generate amide (section 3.2.1), from which reduction occurs to yield the alkylation product **3a** (section 3.2.2).

3.2.1. Acid–Amine Condensation. Detailed Catalyst-Free Mechanism. As mentioned in the Introduction, catalyst-free mechanism includes nucleophilic attack and H₂O-elimination steps.¹⁷ The nucleophilic attack step (Figure 1) starts with the

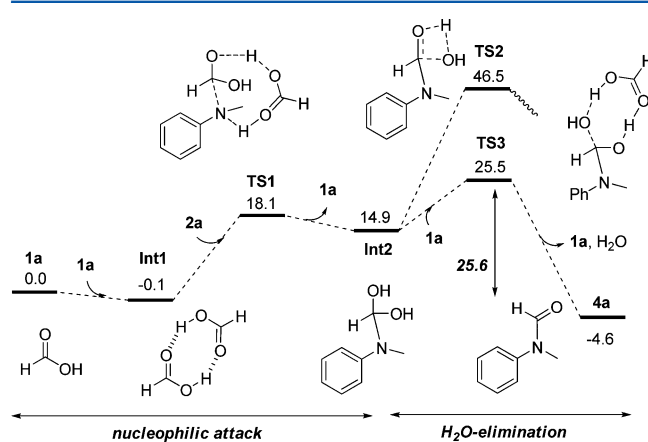


Figure 1. Energy profiles of catalyst-free condensation mechanism (in kcal/mol).

dimerization of carboxylic acid **1a**. The calculation results indicate that the formation of the dimer **Int1** is slightly exergonic by 0.1 kcal/mol, and the two monomers ligate with each other via the hydrogen bonds (Figure 1). After that, the amine substrate **2a** nucleophilically attacks **Int1** via the transition state **TS1** to generate the intermediate **Int2**. In **TS1**, C–N bond formation and the two proton transfer processes (H transfers from O2 to O, H1 transfers from N to

O3, Figure 2) occur simultaneously, and the free energy barrier is 18.2 kcal/mol (**Int1** → **TS1**).

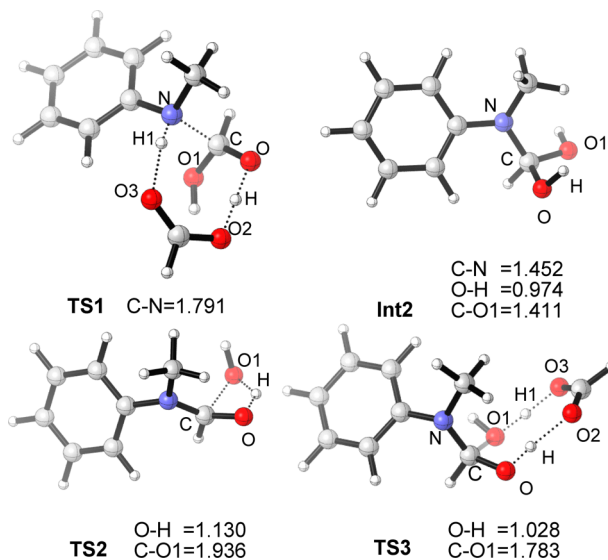


Figure 2. Optimized structures for selected species of catalyst-free mechanism. Bond lengths are given in Ångströms.

For the H₂O-elimination from **Int2**, we first investigated the direct elimination mechanism via the transition state **TS2**. In this transition state, the eliminating H, OH group and the forming carbonyl constitute a four-membered ring. The breaking O–H and C–OH bonds stretch to 1.130 and 1.936 Å in **TS2** from 0.974 and 1.411 Å in **Int2** (Figure 2), respectively. The energy barrier for this step is as high as 46.6 kcal/mol (**Int1** → **TS2**), and thus the possibility for the direct H₂O-elimination can be excluded. Considering that formic acid could possibly act as the proton shuttle,³³ we also examined the energy demand of the indirect H₂O-elimination process. As shown in Figure 1, the two proton transfer processes (H transfers from O to O2, H1 transfers from O3 to O1, Figure 2) and C–O1 cleavage might occur simultaneously via the transition state **TS3**. The breaking O–H bond and C–O1 bond stretch to 1.028 and 1.783 Å, respectively. The free energy barrier of the indirect elimination process is 25.6 kcal/mol (**Int1** → **TS3**), which is much lower than that of the direct elimination (46.6 kcal/mol). The reason may be attributed to the higher acidity of HCOOH than the OH group in **Int2**. After the indirect H₂O-elimination, the amide **4a** was generated. According to the aforementioned discussions, the dimerization-nucleophilic attack-indirect H₂O-elimination represents the feasible catalyst-free condensation mechanism, and the energy demand is 25.6 kcal/mol.

Detailed B(C₆F₅)₃-Catalyzed Mechanism. As mentioned in the Introduction, the condensation might also occur via the silyl ester formation, nucleophilic attack, and HOSiR'₃-elimination steps (B(C₆F₅)₃-catalyzed mechanism). According to the calculation results, the coordination of either substrate **1a** or **2a** to the catalyst B(C₆F₅)₃ can stabilize the boron center (Figure 3A), and the coordination is exergonic by 0.9 or 12.3 kcal/mol, respectively. In addition, the generation of proton-transferred intermediate **12a-B** is exergonic by 11.5 kcal/mol. Therefore, **2a-B** is the main existing form of the catalyst, and was chosen as the starting point of the catalyst B(C₆F₅)₃.

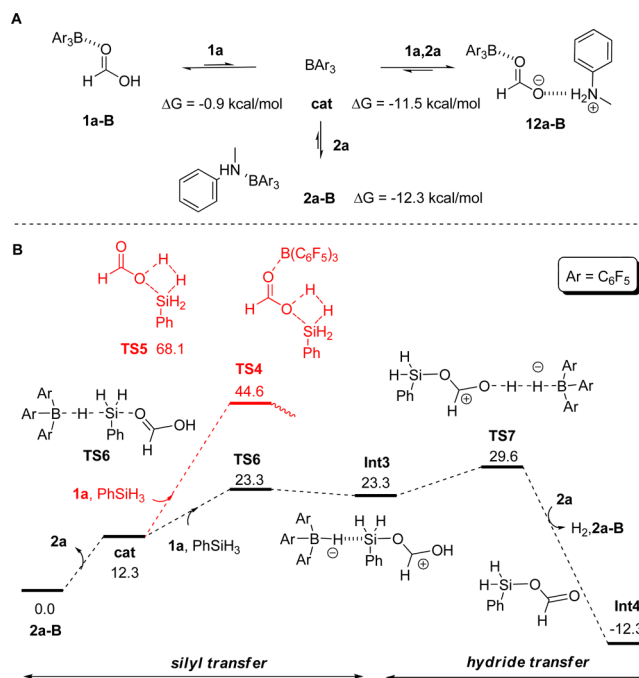


Figure 3. (A) The equilibrium between **cat**, **1a-B**, **2a-B**, and **12a-B**; and (B) the energy profiles of the silyl ester formation process (in kcal/mol).

Figure 3B shows the detailed energy profiles of the silyl ester formation process. The dissociation of **2a** from **2a-B** occurs first to generate the free catalyst **cat**. PhSiH₃ and acid substrate **1a** then participate in the silyl transfer step, and the metathesis-type silyl ester formation was first investigated. In the related transition state **TS4**, the catalyst B(C₆F₅)₃ is coordinated on the carbonyl group of acid, and the breaking O–H of hydroxy and Si–H of PhSiH₃ constitute a four-membered ring. The free energy of **TS4** is 44.6 kcal/mol. For comparison, we also located the similar four-membered cyclic transition state **TS5** without the coordination of B(C₆F₅)₃. The free energy of **TS5** (68.1 kcal/mol) is significantly higher than that of **TS4**, indicating that the Lewis acidity of B(C₆F₅)₃ benefits the cleavage of O–H bond. Nonetheless, both activation barriers are too high to overcome under the experimental conditions (100 °C), and we have to consider the other possibilities.

Inspired by Sakata's recent DFT study^{34a} on B(C₆F₅)₃-catalyzed ketone hydrosilylation, we took into account the possibility of the B(C₆F₅)₃-promoted Si–H cleavage. The energy barrier of the step is 23.3 kcal/mol (**2a-B** → **TS6**). In the optimized structure of **TS6** (Figure 4), the Si–H bond stretches from 1.49 Å (in free PhSiH₃) to 1.58 Å, and the Si–O and B–H bonds shorten to 2.83 and 1.51 Å, respectively. Therefore, we concluded that the breaking of Si–H bond and formation of Si–O and B–H bonds occur simultaneously. In the generated intermediate **Int3**, the Si–O and B–H bonds further shorten to 2.19 and 1.34 Å, and the Si–H distance stretches to 1.69 Å. From **Int3**, hydride transfer³⁴ from the HB(C₆F₅)₃[−] group to the hydroxyl group occurs via the synergistic transition state **TS7**, and the formation of H–H bond and cleavage of O–H and B–H bonds occur simultaneously. This step gives silyl ester intermediate **Int4** and H₂ as the products, and the energy barrier is 29.6 kcal/mol (**2a-B** → **TS7**). The regenerated catalyst B(C₆F₅)₃ then easily coordinates another **2a** to generate the more stable **2a-B**.

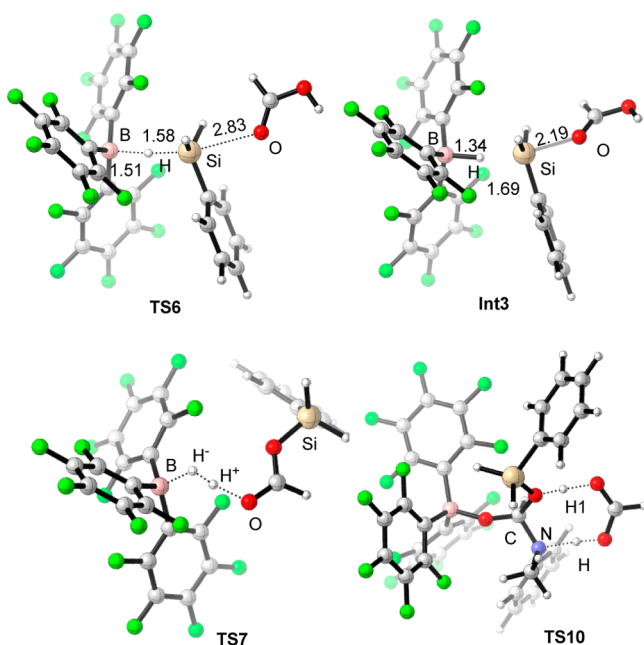


Figure 4. Optimized structures for selected species of $B(C_6F_5)_3$ -catalyzed condensation. Bond lengths are given in angstroms.

From **Int 4**, the energy profiles for the subsequent nucleophilic attack and $HOSiH_2Ph$ -elimination processes are given in **Figure 5**. It is found that the $B(C_6F_5)_3$ exchange between **Int4** and **2a-B** in generating $B(C_6F_5)_3$ -coordinated silyl ester **Int5** is endergonic by 7.7 kcal/mol. After that, nucleophilic attack of **2a** to **Int5** occurs via the transition state **TS8** with an energy barrier of 19.7 kcal/mol (**Int4** \rightarrow **TS8**). This step generates the C–N bond-formed intermediate **Int6**. For the following $HOSiH_2Ph$ -elimination, both the direct elimination and the indirect elimination (with the formic acid as proton shuttle³³) were investigated. For the direct $HOSiH_2Ph$ -elimination process, the free energy of the related four-membered cyclic transition state (i.e., **TS9** in **Figure 5**) is 33.5 kcal/mol. By contrast, with formic acid acting as proton shuttle,

state **TS10** is much lower (i.e., 11.7 kcal/mol, **Figures 4** and **5**). After **TS10**, $HOSiH_2Ph$ is released and the amide **Int7** is formed. The energy barrier of this step is 24.0 kcal/mol (**Int4** \rightarrow **TS10**), and the system energy decreases to -18.1 kcal/mol. According to **Figures 3** and **5**, the energy demand for the $B(C_6F_5)_3$ -catalyzed mechanism is 29.6 kcal/mol (**2a-B** \rightarrow **TS7**).

Comparison between the Catalyst-Free and $B(C_6F_5)_3$ -Catalyzed Condensation Pathways. **Figure 6** shows the comparison between the two possible condensation pathways. For the catalyst-free condensation, nucleophilic attack and H_2O -elimination occur successively to obtain amide **4a** (**Figure 1**). The indirect H_2O -elimination transition state **TS3** is the highest energy-lying species with free energy of 25.5 kcal/mol (**Figure 6**). For the $B(C_6F_5)_3$ -catalyzed condensation, silyl transfer-hydride transfer process first occurs from **2a-B** to give silyl ester **Int4** (**Figure 3**), from which nucleophilic attack and $HOSiH_2Ph$ -elimination occur to obtain **Int7** (**Figure 5**). During these processes, the hydride transfer transition state **TS7** is the highest energy-lying species, and its free energy is 29.6 kcal/mol. Therefore, catalyst-free condensation is more favorable than the $B(C_6F_5)_3$ -catalyzed condensation.

Analyzing the reason for facility of catalyst-free condensation over the $B(C_6F_5)_3$ -catalyzed, we found that the formation of the stable complex **2a-B** is mainly responsible. Without **2a-B**, the energy barrier of $B(C_6F_5)_3$ -catalyzed mechanism is only 17.3 kcal/mol (**2a** \rightarrow **TS7**). However, the formation of **2a-B** is automatic, as long as the boron catalyst is exposed to the amine substrate **2a**. Therefore, the coordination passivates the catalyst, and results in the more feasible catalyst-free condensation mechanism.

3.2.2. Reduction of Amide. Lewis Acid-Catalyzed Reduction. The detailed energy profiles for the Lewis acid-catalyzed reduction have been shown in **Figure 7**. $B(C_6F_5)_3$ exchange first occurs between **4a** and **2a-B** to give $B(C_6F_5)_3$ -coordinated amide **Int7** and **2a**. From **Int7**, the first silyl transfer occurs via the transition state **TS11** to transfer $-SiPhH_2$ group from silane to carbonyl group of the amide. The energy barrier is 28.4 kcal/mol (**Int7** \rightarrow **TS11**). The generated intermediate **Int8** then undergoes hydride transfer transition state **TS12** to transfer H^-

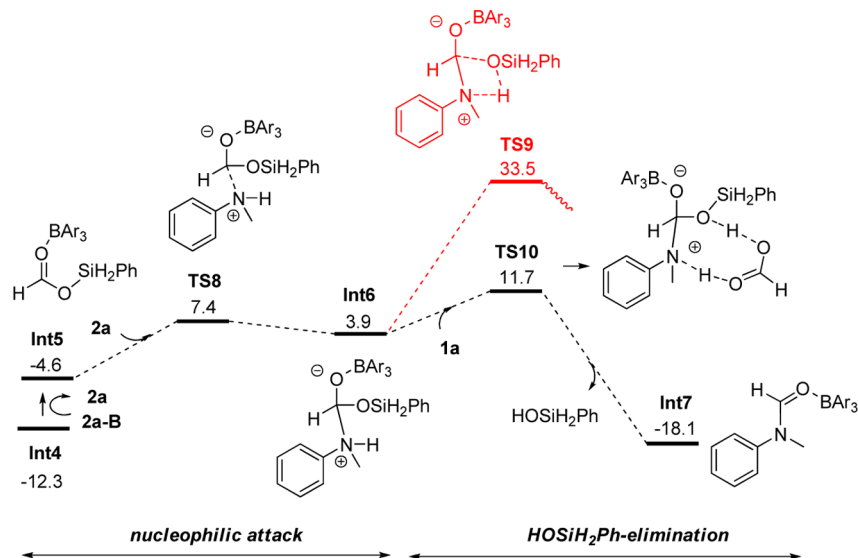


Figure 5. Energy profile of the transformation from silyl ester to amide (in kcal/mol).

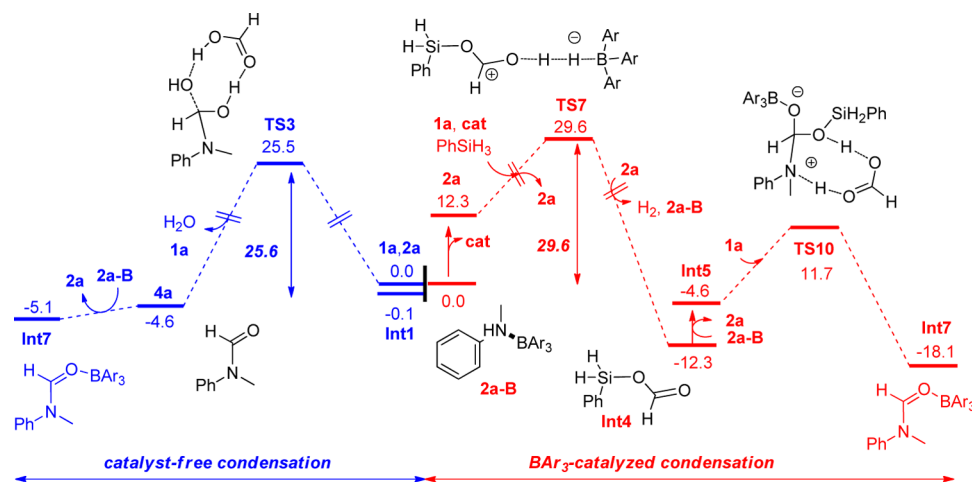


Figure 6. Comparison between the catalyst-free and the $B(C_6F_5)_3$ -catalyzed condensation mechanism.

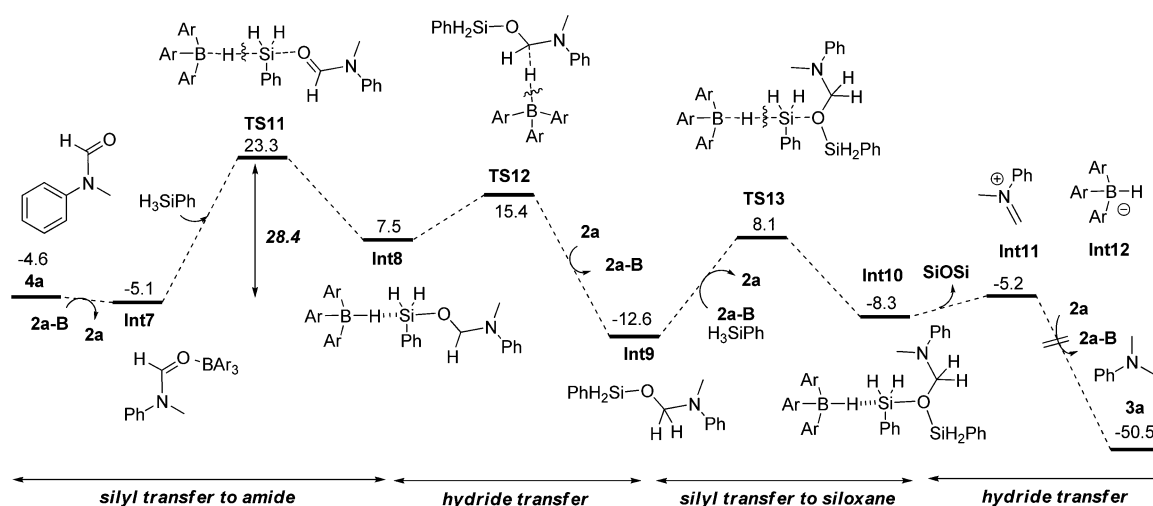


Figure 7. Energy profile of Lewis acid-catalyzed amide reduction (in kcal/mol).

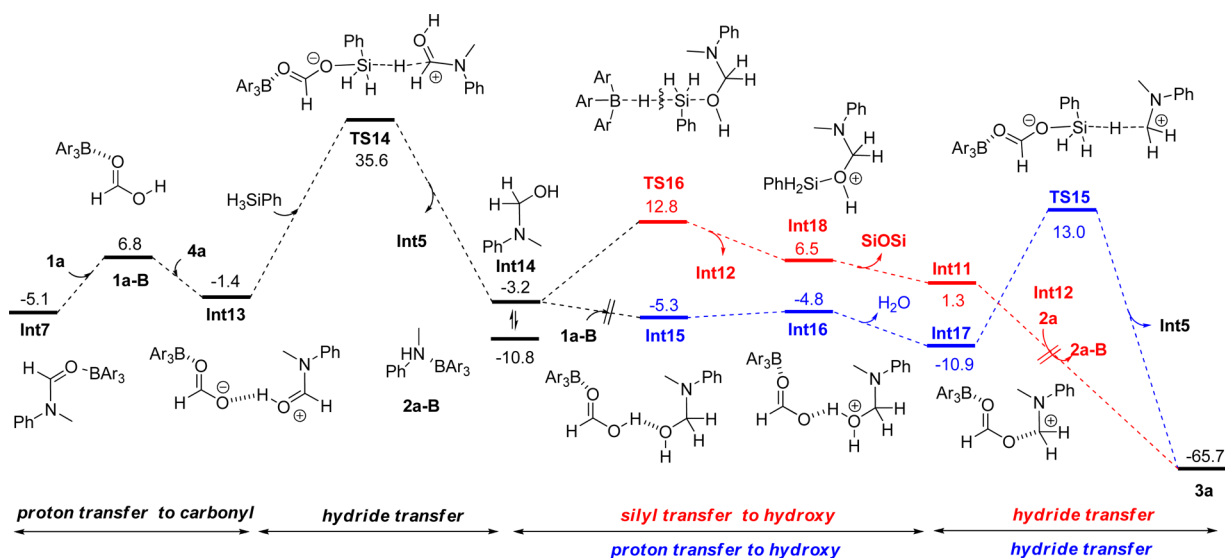


Figure 8. Energy profile of Brønsted acid-catalyzed amide reduction (in kcal/mol).

from $^-HB(C_6F_5)_3$ group to carbonyl C atom, and the energy barrier is 20.5 kcal/mol ($Int7 \rightarrow TS12$). After that, the siloxane intermediate $Int9$ is generated, and the released catalyst is

capped by the amine substrate $2a$. $Int9$ then undergoes $-SiPh_2$ transfer from silane to the O atom of siloxane via the second silyl transfer transition state $TS13$. The generated

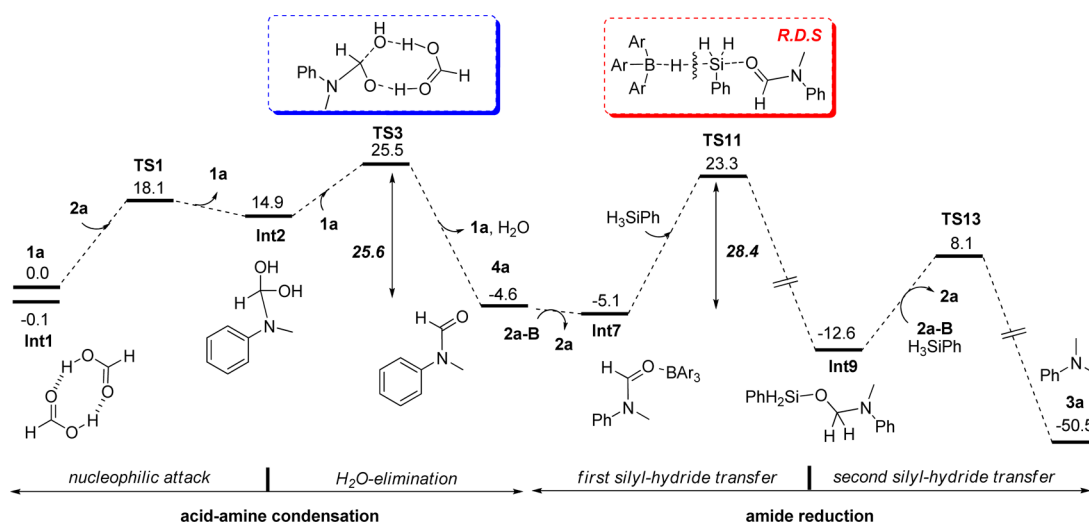


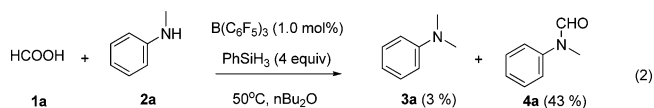
Figure 9. Overall mechanism of the amine alkylation (in kcal/mol).

intermediate **Int10** then easily dissociates SiOSi ($\text{PhH}_2\text{SiOSiPhH}_2$) to generate the imine cation **Int11** and the anion intermediate **Int12**. Finally, a facile hydride transfer occurs between these two intermediates to generate alkylation product **3a** with the regeneration of **2a-B**. According to Figure 7, the first silyl transfer transition state **TS11** determines the overall energy demand of the amide reduction process (28.4 kcal/mol, **Int7** \rightarrow **TS11**).

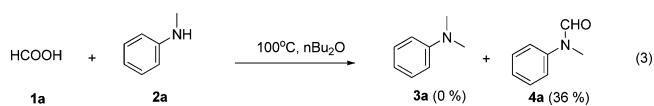
Brønsted Acid-Catalyzed Reduction. Figure 8 shows the detailed energy profiles for the Brønsted acid-catalyzed amide reduction. $\text{B}(\text{C}_6\text{F}_5)_3$ first transfers from **Int7** to **1a**, giving $\text{B}(\text{C}_6\text{F}_5)_3$ -coordinated acid **1a-B** as the product. The process is endergonic by 11.9 kcal/mol, because amide is more nucleophilic than acid. The proton in **1a-B** then transfers to the O atom in **4a** to generate **Int13**. The process is barrierless with an energy decrease of 8.2 kcal/mol. Subsequently, with the participation of silane, hydride transfer occurs via the transition states **TS14**. In **TS14**, the COO^- group nucleophilically attacks the Si atom of silane, and the hydride of silane transfers to the carbon cation. The energy barrier of the elementary hydride transfer step is 37.0 kcal/mol (**Int13** \rightarrow **TS14**). After this step, $\text{B}(\text{C}_6\text{F}_5)_3$ -coordinated silyl ester **Int5** and **Int14** are generated with an energy decrease of 38.8 kcal/mol. Thereafter, two mechanisms might be responsible for the reduction of **Int14** to the product **3a** (Figure 8). In the Brønsted acid-catalyzed reduction (in blue), the proton transfer in intermediate **Int15** first occurs to generate **Int16**. With the release of H_2O , **Int17** is generated with an energy decrease of 6.1 kcal/mol. The silane-mediated hydride transfer then occurs via the transition state **TS15**. The energy barrier of this step is 23.9 kcal/mol. The product **3a** is finally yielded with **Int5**. In the Lewis acid (i.e., $\text{B}(\text{C}_6\text{F}_5)_3$)-catalyzed reduction (in red), **Int14** first goes through a silyl transfer transition state **TS16** to generate the intermediate **Int18**. The **Int18** dissociates SiOSi to give cation **Int11**. The facile hydride transfer occurs between **Int11** and **Int12** to obtain **3a** and regenerate **2a-B**. The energy barrier of this mechanism is 23.7 kcal/mol (**Int17** \rightarrow **TS16**). Therefore, for the reduction of **Int14**, both of these mechanisms are possible (23.9 vs 23.7 kcal/mol). For the overall Brønsted acid-catalyzed amide reduction, the first hydride transfer transition state **TS14** determines the overall energy barrier (40.7 kcal/mol, **Int7** \rightarrow **TS14**). It is unfavorable as compared to the Lewis acid-catalyzed one (28.4 kcal/mol, Figure 7).

3.3. Overall Mechanism of Amine Alkylation. For clarity reasons, the overall mechanism of the $\text{B}(\text{C}_6\text{F}_5)_3$ -catalyzed amine alkylation is shown in Figure 9. The acid **1a** and amine **2a** first undergo the catalyst-free condensation (including nucleophilic attack and H_2O -elimination) to generate amide **4a**. The H_2O -elimination step determines the energy demand of the condensation (25.6 kcal/mol). The following amide reduction undergoes twice silyl transfer-hydride transfer processes to generate alkylation product **3a**. The first silyl transfer determines the energy demand of the amide reduction (28.4 kcal/mol). According to these results, the first silyl transfer in amide reduction is the rate-determining step of the amine alkylation reaction, and the overall activation barrier is 28.4 kcal/mol.

To verify the above calculation results, some experiments were carried out. First, condensation product amide was mainly obtained under a lowered temperature (eq 2), and this



observation is consistent with the calculation results that acid-amine condensation is easier than the amide reduction. Second, without the catalyst $\text{B}(\text{C}_6\text{F}_5)_3$ and reductant PhSiH_3 , the reaction of **1a** and **2a** gives amide **4a** as the product (eq 3), and this is consistent with the catalyst-free condensation mechanism.³⁵



3.4. Discussions on Acid Reduction Mechanism. According to the previous studies by Yamamoto^{18a} and Brookhart,^{18b} the carboxylic acid could be reduced to disilyl acetal under the $\text{B}(\text{C}_6\text{F}_5)_3$ -silane system.¹⁸ Note that our reaction system is highly similar to Yamamoto's, whereas no disilyl acetal was obtained. To explore the origin of the interesting chemoselectivity, we carried out the following calculations and discussions.

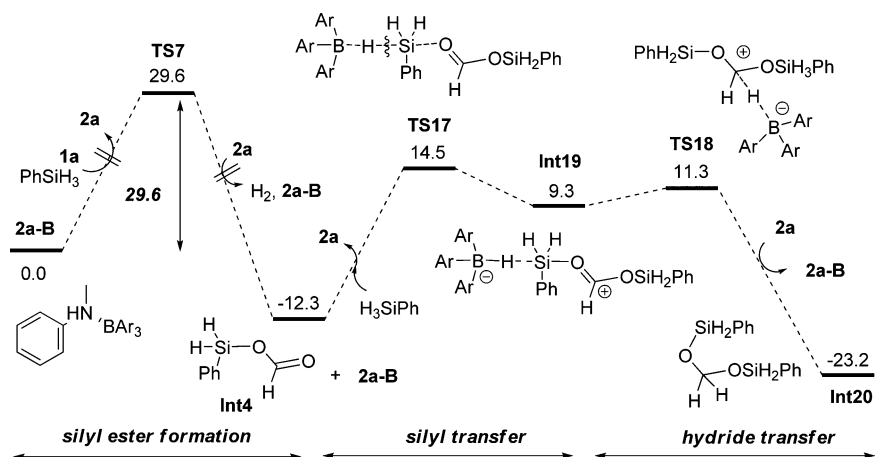


Figure 10. Energy profile of acid reduction process (in kcal/mol).

In our system, the carboxylic acid could be first reduced to the silyl ester ($2a-B + 1a + \text{PhSiH}_3 \rightarrow \text{Int4}$, as shown in Figure 3B), and then the second reduction can occur to obtain the disilyl acetal. The energy barrier for the transformation of **1a** to silyl ester **Int4** is 29.6 kcal/mol. From **Int4**, silyl transfer occurs via transition state **TS17**, transferring the silyl group from silane to the carbonyl in **Int4** to generate intermediate **Int19**. The free energy barrier of this step is 26.8 kcal/mol (**Int4** \rightarrow **TS17**). Next, **Int19** undergoes the hydride transfer step to give the disilyl acetal **Int20** via the transition state **TS18**. The free energy barrier of this step is 23.6 kcal/mol (**Int4** \rightarrow **TS18**). Accordingly, the transformation from **1a** to **Int20** undergoes twice silyl transfer-hydride transfer processes. The first hydride transfer transition state **TS7** determines the overall energy barrier (29.6 kcal/mol).

Comparing the acid reduction (Figure 10) with amine alkylation (Figure 7), we found that the amide **4a** would be facily generated, because the acid–amine condensation is stoichiometric and has a lower energy barrier than the acid reduction (25.6 vs 29.6 kcal/mol). From **4a**, the energy barrier of amide reduction is still lower than that of acid reduction (28.4 vs 29.6 kcal/mol). Therefore, the amine alkylation is kinetically more favorable than acid reduction, which is consistent with our previous experiments that alkylation product was obtained predominantly. In addition, the origin of the chemoselectivity is the same as the selectivity origin of the catalyst-free condensation mechanism (over the $\text{B}(\text{C}_6\text{F}_5)_3$ -catalyzed one). That is, the formation of the stable amine– $\text{B}(\text{C}_6\text{F}_5)_3$ complex (**2a-B**) passivates the catalyst and results in the unfavorable $\text{B}(\text{C}_6\text{F}_5)_3$ -catalyzed acid reduction.

4. CONCLUSIONS

Our group recently reported the $\text{B}(\text{C}_6\text{F}_5)_3$ -catalyzed carboxylic acid-participated alkylation of various aromatic and aliphatic amines with silane as reductant. In the present study, DFT calculations were carried out to investigate the detailed mechanism. The calculation results show that the condensation of amine and acid undergoes with a catalyst-free mechanism rather than a $\text{B}(\text{C}_6\text{F}_5)_3$ -catalyzed mechanism. For the catalyst-free condensation, nucleophilic attack of amine to acid occurs prior to the H_2O -elimination, and an indirect elimination process with acid as the proton shuttle is the favorable H_2O -elimination mechanism. The following amide reduction undergoes Lewis acid ($\text{B}(\text{C}_6\text{F}_5)_3$)-catalyzed mechanism rather than the Brønsted acid ($\text{B}(\text{C}_6\text{F}_5)_3$ -coordinated HCOOH)-catalyzed

one. The favorable reduction process includes twice silyl transfer-hydride transfer processes to obtain the alkylation product, with the first silyl transfer acting as the rate-determining step of the overall alkylation process. The alkylation mechanism is supported by the control experiments of temperature and substrates. Finally, the catalyst passivation caused by the automatic coordination of amine with $\text{B}(\text{C}_6\text{F}_5)_3$ catalyst is determinant to the chemoselectivity, because it results in the unfavorable acid reduction step and the associated $\text{B}(\text{C}_6\text{F}_5)_3$ -catalyzed acid reduction mechanisms.

5. EXPERIMENTAL SECTION

General Procedure. In a Schlenk tube under argon atmosphere, $\text{B}(\text{C}_6\text{F}_5)_3$ (1.0 mol %, 1.1 mg) was dissolved in dry $^t\text{Bu}_2\text{O}$ (1.0 mL), and PhSiH_3 (4.0 equiv) was added. Next, *N*-methylaniline (1.0 equiv, 0.2 mmol) and HCO_2H (2.3 equiv, 4.6 mmol) were added via a syringe. The reaction mixture was stirred for 8 h at 100 °C. After completion, the mixture was diluted with ethyl acetate (5 mL), quenched with aqueous NaOH (3 M solution; 3 mL) carefully, and stirred for 3 h at room temperature. The yields were analyzed by GC using *n*-dodecane as an internal standard.

***N,N*-Dimethylaniline (3a).** The compound data were in agreement with the literature (*Adv. Synth. Catal.* **2015**, 357, 714). ^1H NMR (400 MHz, CDCl_3): δ 7.29–7.19 (m, 2H), 7.02–6.34 (m, 3H), 2.94 (s, 6H).

***N*-Methylformanilide (4a).** The compound data were in agreement with the literature (*Chem. Commun.* **2014**, 50, 189). ^1H NMR (400 MHz, CDCl_3): δ 8.48 (s, 1H), 7.42 (t, $J = 7.9$ Hz, 1H), 7.35–7.26 (m, 1H), 7.22–7.15 (m, 1H), 3.33 (s, 1H).

■ ASSOCIATED CONTENT

Supporting Information

The Supporting Information is available free of charge on the ACS Publications website at DOI: 10.1021/acs.joc.6b00778.

Details of the control experiments, and Cartesian coordinates, free energies, and thermal corrections (PDF)

■ AUTHOR INFORMATION

Corresponding Authors

*E-mail: yuhaizhu@ahu.edu.cn.

*E-mail: fuyao@ustc.edu.cn.

Notes

The authors declare no competing financial interest.

ACKNOWLEDGMENTS

This work was supported by the 973 Program (2012CB215305), NSFC (21325208, 21402181, 21572212), IPDFHCPST (2014FXCX006), CAS (KFJ-EW-STS-051, YZ201563), FRFCU, PCSIRT, and the National Supercomputing Center in Shenzhen and USTC for providing the computational resources.

REFERENCES

- (1) (a) Nugent, T. C.; El-Shazly, M. *Adv. Synth. Catal.* **2010**, *352*, 753. (b) Wolfe, J. P.; Wagav, S.; Marcoux, J. F.; Buchwald, S. L. *Acc. Chem. Res.* **1998**, *31*, 805.
- (2) For reviews, see: (a) Ramirez, T. A.; Zhao, B.; Shi, Y. *Chem. Soc. Rev.* **2012**, *41*, 931. (b) Yadav, J. S.; Antony, A.; Rao, T. S.; Reddy, B. V. S. *J. Organomet. Chem.* **2011**, *696*, 16. (c) Crozet, D.; Urrutigoity, M.; Kalcik, P. *ChemCatChem* **2011**, *3*, 1102. (d) Bähn, S.; Imm, S.; Neubert, L.; Zhang, M.; Neumann, H.; Beller, M. *ChemCatChem* **2011**, *3*, 1853. (e) Collet, F.; Lescot, C.; Dauban, P. *Chem. Soc. Rev.* **2011**, *40*, 1926. (f) Guillena, G.; Ramon, D. J.; Yus, M. *Chem. Rev.* **2010**, *110*, 1611. (g) Mueller, T. E.; Hultsch, K. C.; Yus, M.; Foubelo, F.; Tada, M. *Chem. Rev.* **2008**, *108*, 3795. (h) Beauchemin, A. M.; Moran, J.; Lebrun, M.-E.; Seguin, C.; Dimitrijevic, E.; Zhang, L.; Gorelsky, S. I. *Angew. Chem., Int. Ed.* **2008**, *47*, 1410. (i) Salvatore, R. N.; Yoon, C. H.; Jung, K. W. *Tetrahedron* **2001**, *57*, 7785.
- (3) (a) *Modern Amination Methods*; Ricci, A., Ed.; Wiley-VCH: Weinheim, 2007. (b) *Advanced Organic Chemistry*, 5th ed.; Smith, M. B., March, J., Eds.; Wiley-Interscience: New York, 2001.
- (4) For reviews, see: (a) Werkmeister, S.; Junge, K.; Beller, M. *Org. Process Res. Dev.* **2014**, *18*, 289. (b) Bezier, D.; Sortais, J.-B.; Darcel, C. *Adv. Synth. Catal.* **2013**, *355*, 19. (c) Xie, J.-H.; Zhu, S.-F.; Zhou, Q.-L. *Chem. Rev.* **2011**, *111*, 1713. (d) Addis, D.; Das, S.; Junge, K.; Beller, M. *Angew. Chem., Int. Ed.* **2011**, *50*, 6004. (e) Nugent, T. C.; El-Shazly, M. *Adv. Synth. Catal.* **2010**, *352*, 753. (f) Das, S.; Zhou, S.; Addis, D.; Enthaler, S.; Junge, K.; Beller, M. *Top. Catal.* **2010**, *53*, 979. (g) Kobayashi, S.; Ishitani, H. *Chem. Rev.* **1999**, *99*, 1069.
- (5) (a) Patureau, F. W.; Boer, S. D.; Kuil, M.; Meeuwissen, J.; Breuil, P.-A. R.; Siegler, M. A.; Spek, A. L.; Sandee, A. J.; Bruin, B. D.; Reek, J. N. H. *J. Am. Chem. Soc.* **2009**, *131*, 6683. (b) Gridnev, I. D.; Imamoto, T.; Hoge, G.; Kouchi, M.; Takahashi, H. *J. Am. Chem. Soc.* **2008**, *130*, 2560. (c) Wang, D.-Y.; Hu, X.-P.; Huang, J.-D.; Deng, J.; Yu, S.-B.; Duan, Z.-C.; Xu, X.-F.; Zheng, Z. *Angew. Chem., Int. Ed.* **2007**, *46*, 7810. (d) Shang, G.; Yang, Q.; Zhang, X. *Angew. Chem., Int. Ed.* **2006**, *45*, 6360. (e) Hou, G.-H.; Xie, J.-H.; Wang, L.-X.; Zhou, Q.-L. *J. Am. Chem. Soc.* **2006**, *128*, 11774. (f) Burk, M. J.; Wang, Y. M.; Lee, J. R. *J. Am. Chem. Soc.* **1996**, *118*, 5142 and references cited therein.
- (6) (a) Hou, G.-H.; Xie, J.-H.; Yan, P.-C.; Zhou, Q.-L. *J. Am. Chem. Soc.* **2009**, *131*, 1366. (b) Han, Z.; Wang, Z.; Zhang, X.; Ding, K. *Angew. Chem., Int. Ed.* **2009**, *48*, 5345. (c) Erre, G. E.; Enthaler, S.; Junge, K.; Addis, D.; Beller, M. *Adv. Synth. Catal.* **2009**, *351*, 1437. (d) Zhu, S.-F.; Xie, J.-B.; Zhang, Y.-Z.; Li, S.; Zhou, Q.-L. *J. Am. Chem. Soc.* **2006**, *128*, 12886. (e) Moessner, C.; Bolm, C. *Angew. Chem., Int. Ed.* **2005**, *44*, 7564. (f) Maire, P.; Deblon, S.; Breher, F.; Geier, J.; Böhrer, C.; Rügger, H.; Schönberg, H.; Grützmacher, H. *Chem. - Eur. J.* **2004**, *10*, 4198. (g) Solinas, M.; Pfaltz, A.; Cozzi, P. G.; Leitner, W. *J. Am. Chem. Soc.* **2004**, *126*, 16142.
- (7) (a) Cheruku, P.; Church, T. L.; Andersson, P. G. *Chem. - Asian J.* **2008**, *3*, 1390. (b) Clarke, M. L.; Diaz-Valenzuela, B.; Slawin, A. M. *Organometallics* **2007**, *26*, 16. (c) Cogley, C. J.; Henschke, J. P. *Adv. Synth. Catal.* **2003**, *345*, 195. (d) Dupau, P.; Bruneau, C.; Dixneuf, P. H. *Adv. Synth. Catal.* **2001**, *343*, 331. (e) Abdur-Rashid, K.; Lough, A. J.; Morris, R. H. *Organometallics* **2001**, *20*, 1047. (f) Noyori, R.; Ohta, M.; Hsiao, Y.; Kitamura, M.; Ohta, T.; Takaya, H. *J. Am. Chem. Soc.* **1986**, *108*, 7117 and references cited therein.
- (8) (a) Yu, C.-B.; Wang, D.-W.; Zhou, Y.-G. *J. Org. Chem.* **2009**, *74*, 5633. (b) Wang, Y.-Q.; Yu, C.-B.; Wang, D.-W.; Wang, X.-B.; Zhou, Y.-G. *Org. Lett.* **2008**, *10*, 2071. (c) Wang, Y.-Q.; Lu, S.-M.; Zhou, Y.-G. *J. Org. Chem.* **2007**, *72*, 3729. (d) Yang, Q.; Shang, G.; Gao, W.; Deng, J.; Zhang, X. *Angew. Chem., Int. Ed.* **2006**, *45*, 3832. (e) Suzuki, A.; Mae, M.; Amii, H.; Uneyama, K. *J. Org. Chem.* **2004**, *69*, 5132. (f) Abe, H.; Amii, H.; Uneyama, K. *Org. Lett.* **2001**, *3*, 313.
- (9) (a) Chusov, D.; List, B. *Angew. Chem., Int. Ed.* **2014**, *53*, 5199. (b) Kadyrov, R.; Riermeier, T. H.; Dingerdissen, U.; Tararov, V.; Börner, A. *J. Org. Chem.* **2003**, *68*, 4067. (c) Tararov, V. I.; Kadyrov, R.; Riermeier, T. H.; Börner, A. *Chem. Commun.* **2000**, 1867. (d) Margalef-Català, R.; Claver, C.; Salagre, P.; Fernández, E. *Tetrahedron Lett.* **2000**, *41*, 6583.
- (10) (a) Gnanamgari, D.; Moores, A.; Rajaseelan, E.; Crabtree, R. H. *Organometallics* **2007**, *26*, 1226. (b) Mizuta, T.; Sakaguchi, S.; Ishii, Y. *J. Org. Chem.* **2005**, *70*, 2195. (c) Imao, D.; Fujihara, S.; Yamamoto, T.; Ohta, T.; Ito, Y. *Tetrahedron* **2005**, *61*, 6988. (d) Chi, Y.; Zhou, Y.-G.; Zhang, X. *J. Org. Chem.* **2003**, *68*, 4120.
- (11) (a) Li, Y.; Fang, X.; Junge, K.; Beller, M. *Angew. Chem., Int. Ed.* **2013**, *52*, 9568. (b) Beydoun, K.; Stein, T. V.; Klankermayer, J.; Leitner, W. *Angew. Chem., Int. Ed.* **2013**, *52*, 9554. (c) Li, Y.; Sorribes, I.; Yan, T.; Junge, K.; Beller, M. *Angew. Chem., Int. Ed.* **2013**, *52*, 12156. (d) Kadyrov, R.; Riermeier, T. H. *Angew. Chem., Int. Ed.* **2003**, *42*, 5472.
- (12) (a) Bernardo, J. R.; Sousa, S. C. A.; Florindo, P. R.; Wolff, M.; Machura, B.; Fernandes, A. C. *Tetrahedron* **2013**, *69*, 9145. (b) Das, B. G.; Ghorai, P. *Chem. Commun.* **2012**, *48*, 8276.
- (13) (a) Jaafar, H.; Li, H.; Castro, L. C. M.; Zheng, J.; Roisnel, T.; Dorcet, V.; Sortais, J.-B.; Darcel, C. *Eur. J. Inorg. Chem.* **2012**, *2012*, 3546. (b) Enthaler, S. *ChemCatChem* **2010**, *2*, 1411.
- (14) (a) Sorribes, I.; Junge, K.; Beller, M. *Chem. - Eur. J.* **2014**, *20*, 7878. (b) Jacquet, O.; Frogneux, X.; Gomes, C. D. N.; Cantat, T. *Chem. Sci.* **2013**, *4*, 2127. (c) Kumar, V.; Sharma, U.; Verma, P. K.; Kumar, N.; Singh, B. *Adv. Synth. Catal.* **2012**, *354*, 870. (d) Sreedhar, B.; Reddy, P. S.; Devi, D. K. *J. Org. Chem.* **2009**, *74*, 8806. (e) Lee, O.-Y.; Law, K.-L.; Ho, C.-Y.; Yang, D. *J. Org. Chem.* **2008**, *73*, 8829. (f) Robichaud, A.; Ajjau, A. N. *Tetrahedron Lett.* **2006**, *47*, 3633 and references cited therein.
- (15) Sorribes, I.; Junge, K.; Beller, M. *J. Am. Chem. Soc.* **2014**, *136*, 14314.
- (16) Fu, M.-C.; Shang, R.; Cheng, W.-M.; Fu, Y. *Angew. Chem., Int. Ed.* **2015**, *54*, 9042.
- (17) Charville, H.; Jackson, D. A.; Hodges, G.; Whiting, A.; Wilson, M. R. *Eur. J. Org. Chem.* **2011**, *2011*, 5981.
- (18) (a) Gevorgyan, V.; Rubin, M.; Liu, J. X.; Yamamoto, Y. *J. Org. Chem.* **2001**, *66*, 1672. (b) Bézier, D.; Park, S.; Brookhart, M. *Org. Lett.* **2013**, *15*, 496. (c) Feghali, E.; Jacquet, O.; Thuéry, P.; Cantat, T. *Catal. Sci. Technol.* **2014**, *4*, 2230.
- (19) The review for frustrated Lewis pair: (a) Stephan, D. W.; Erker, G. *Angew. Chem., Int. Ed.* **2015**, *54*, 6400. (b) Stephan, D. W. *Acc. Chem. Res.* **2015**, *48*, 306.
- (20) Blondiaux, E.; Cantat, T. *Chem. Commun.* **2014**, *50*, 9349.
- (21) Parks, D. J.; Blackwell, J. M.; Piers, W. E. *J. Org. Chem.* **2000**, *65*, 3090.
- (22) Rubin, M.; Schwier, T.; Gevorgyan, V. *J. Org. Chem.* **2002**, *67*, 1936.
- (23) (a) Doyle, M. P.; DeBruyn, D. J.; Kooistra, D. A. *J. Am. Chem. Soc.* **1972**, *94*, 3659. (b) West, C. T.; Donnelly, S.; Kooistra, D. A.; Doyle, M. P. *J. Org. Chem.* **1973**, *38*, 2675. (c) Doyle, M. P.; West, C. T. *J. Org. Chem.* **1975**, *40*, 3835.
- (24) (a) Sassaman, M. B.; Kotian, K. D.; Prakash, G. K. S.; Olah, G. A. *J. Org. Chem.* **1987**, *52*, 4314. (b) Sassaman, M. B.; Prakash, G. K. S.; Olah, G. A. *Tetrahedron* **1988**, *44*, 3771.
- (25) Frisch, M. J.; Trucks, G. W.; Schlegel, H. B.; Scuseria, G. E.; Robb, M. A.; Cheeseman, J. R.; Scalmani, G.; Barone, V.; Mennucci, B.; Petersson, G. A.; Nakatsuji, H.; Caricato, M.; Li, X.; Hratchian, H. P.; Izmaylov, A. F.; Bloino, J.; Zheng, G.; Sonnenberg, J. L.; Hada, M.; Ehara, M.; Toyota, K.; Fukuda, R.; Hasegawa, J.; Ishida, M.; Nakajima, T.; Honda, Y.; Kitao, O.; Nakai, H.; Vreven, T.; Montgomery, J. A., Jr.; Peralta, J. E.; Ogliaro, F.; Bearpark, M.; Heyd, J. J.; Brothers, E.; Kudin, K. N.; Staroverov, V. N.; Keith, T.; Kobayashi, R.; Normand, J.; Raghavachari, K.; Rendell, A.; Burant, J. C.; Iyengar, S. S.; Tomasi, J.; Cossi, M.; Rega, N.; Millam, J. M.; Klene, M.; Knox, J. E.; Cross, J. B.; Bakken, V.; Adamo, C.; Jaramillo, J.; Gomperts, R.; Stratmann, R. E.;

Yazyev, O.; Austin, A. J.; Cammi, R.; Pomelli, C.; Ochterski, J. W.; Martin, R. L.; Morokuma, K.; Zakrzewski, V. G.; Voth, G. A.; Salvador, P.; Dannenberg, J. J.; Dapprich, S.; Daniels, A. D.; Farkas, O.; Foresman, J. B.; Ortiz, J. V.; Cioslowski, J.; Fox, D. J. *Gaussian 09*, revision D.01; Gaussian, Inc.: Wallingford, CT, 2013.

- (26) Becke, A. D. *J. Chem. Phys.* **1993**, *98*, 5648.
- (27) Lee, C.; Yang, W.; Parr, R. G. *Phys. Rev. B: Condens. Matter Mater. Phys.* **1988**, *37*, 785.
- (28) (a) Zhao, H.-T.; Lin, Z.-Y.; Marder, T. B. *J. Am. Chem. Soc.* **2006**, *128*, 15637. (b) Liu, B.; Gao, M.; Dang, L.; Zhao, H.-T.; Marder, T. B.; Lin, Z.-Y. *Organometallics* **2012**, *31*, 3410. (c) Kleeberg, C.; Crawford, A. G.; Batsanov, A. S.; Hodgkinson, P.; Apperley, D. C.; Cheung, M. S.; Lin, Z.-Y.; Marder, T. B. *J. Org. Chem.* **2012**, *77*, 785. (d) Paddon-Row, M. N.; Anderson, C. D.; Houk, K. N. *J. Org. Chem.* **2009**, *74*, 861. (e) Zhang, Q.; Yu, H.-Z.; Shi, J. *Acta Phys.-Chim. Sin.* **2013**, *29*, 2321. (f) Zhang, Q.; Yu, H.-Z.; Fu, Y. *Org. Chem. Front.* **2014**, *1*, 614. (g) Li, Z.; Liu, L. *Chin. J. Catal.* **2015**, *36*, 3. (h) Shang, R.; Yang, Z.-W.; Wang, Y.; Zhang, S.-L.; Liu, L. *J. Am. Chem. Soc.* **2010**, *132*, 14391.
- (29) Hollwarth, A.; Bohme, M.; Dapprich, S.; Ehlers, A. W.; Gobbi, A.; Jonas, V.; Kohler, K. F.; Stegmann, R.; Veldkamp, A.; Frenking, G. *Chem. Phys. Lett.* **1993**, *208*, 237.
- (30) Gonzalez, C.; Schlegel, H. B. *J. Phys. Chem.* **1990**, *94*, 5523.
- (31) (a) Zhao, Y.; Truhlar, D. G. *Theor. Chem. Acc.* **2008**, *120*, 215. (b) Zhao, Y.; Truhlar, D. G. *Acc. Chem. Res.* **2008**, *41*, 157.
- (32) B3LYP//M06-2X method has been frequently used in theoretical studies of organic reaction systems: (a) Um, J. M.; DiRocco, D. A.; Noey, E. L.; Rovis, T.; Houk, K. N. *J. Am. Chem. Soc.* **2011**, *133*, 11249. (b) Krenske, E. H.; Houk, K. N.; Harmata, M. *J. Org. Chem.* **2015**, *80*, 744. (c) Xue, X.-S.; Yang, C.; Li, X.; Cheng, J.-P. *J. Org. Chem.* **2014**, *79*, 1166. (d) McIntosh, G. J.; Russell, D. K. *J. Phys. Chem. A* **2013**, *117*, 4183. (e) Lo, R.; Ganguly, B. *J. Phys. Chem. C* **2013**, *117*, 19325. (f) Flynn, B. L.; Manchala, N.; Krenske, E. H. *J. Am. Chem. Soc.* **2013**, *135*, 9156. (g) McIntosh, G. J.; Russell, D. K. *J. Phys. Chem. A* **2014**, *118*, 12192.
- (33) (a) Qu, S.; Dang, Y.; Song, C.; Guo, J.; Wang, Z.-X. *ACS Catal.* **2015**, *5*, 6386. (b) Clark, J. M.; Nimlos, M. R.; Robichaud, D. J. *J. Phys. Chem. A* **2015**, *119*, 501.
- (34) (a) Sakata, K.; Fujimoto, H. *J. Org. Chem.* **2013**, *78*, 12505. (b) Houghton, A. Y.; Hurmalainen, J.; Mansikkamäki, A.; Piers, W. E.; Tuononen, H. M. *Nat. Chem.* **2014**, *6*, 983.
- (35) Please see the [Supporting Information](#) for the experimental details.